Int Urol Nephrol
DOI 10.1007/s11255-015-1194-7

NEPHROLOGY - ORIGINAL PAPER

Ultrasound findings in EHEC-associated hemolytic-uremic syndrome and their clinical relevance

Ansgar Reising[1] · Carsten Hafer[1,2] · Marcus Hiss[1] · Jan T. Kielstein[1,3] · Jan Menne[1] · Faikah Gueler[1] · Jan Beneke[1] · Silvia Linnenweber-Held[1] · Hermann Haller[1] · Gunilla Einecke[1]

Received: 21 September 2015 / Accepted: 18 December 2015

Abstract
Purpose Hemolytic-uremic syndrome (HUS) and acute kidney injury (AKI) after infection with Shiga toxin-producing *E. coli* (EHEC) are clinically important complications. We present a retrospective analysis of abdominal ultrasound findings in patients with HUS caused by EHEC O104:H4 ($n = 41$).
Methods We assessed intrarenal resistance indices and quantitated kidney parenchymal density by the kidney/liver intensity ratio using computer-based image analysis. Findings in EHEC–HUS were compared to those in AKI due to other reasons ($n = 60$) and 19 healthy volunteers.
Results Kidneys in EHEC–HUS patients showed severe morphologic changes with striking parenchymal echogenicity. Renal resistance index was increased in HUS (0.80 ± 0.08) compared to patients with AKI due to glomerulopathy (0.69 ± 0.08, $p < 0.001$) or patients with other causes of AKI (0.74 ± 0.10, $p < 0.01$). Parenchymal density was increased in EHEC–HUS (1.39 ± 0.35) compared to AKI due to glomerulopathy (1.18 ± 0.20, $p < 0.05$), other causes of AKI (1.12 ± 0.21, $p < 0.001$) and healthy controls (0.86 ± 0.16, $p < 0.001$). Patients with atypical HUS showed increased parenchymal density (1.43 ± 0.37), similar to those with EHEC–HUS. EHEC–HUS patients who required dialysis treatment had higher parenchymal density (1.58 ± 0.08) compared to those without dialysis (1.14 ± 0.05, $p = 0.0004$). Extrarenal findings in EHEC–HUS included hepatomegaly (45 %), splenomegaly (39 %), ascites (84 %) and pleural effusions (84 %).
Conclusions Patients with EHEC–HUS had a characteristic constellation of morphologic abnormalities on ultrasound examination, indicating that the effects of HUS are not limited to the kidney but include multiple organs, possibly mediated through systemic capillary leakage. Assessment of parenchymal echogenicity contributes to the differential diagnosis of AKI. Parameters reflecting renal perfusion correlated with severity of disease and thus may have prognostic value in future patient evaluation.

Keywords Acute kidney injury · EHEC · Hemolytic-uremic syndrome · Image analysis · Resistance index · Ultrasound

Abbreviations

HUS	Hemolytic-uremic syndrome
RI	Resistance index
AKI	Acute kidney injury

Introduction

Acute kidney injury (AKI) is a common finding among hospitalized patients with increasing incidence. It is associated with high morbidity and mortality [1]. Causes of AKI vary and may range from reduced kidney perfusion and prerenal AKI to direct intrarenal injury and urinary tract obstruction. While the final consequences are similar, i.e.,

Ansgar Reising and Carsten Hafer have contributed equally to this paper.

✉ Ansgar Reising
reising.ansgar@mh-hannover.de

[1] Department of Nephrology and Hypertension, Hannover Medical School, Carl-Neuberg-Str. 1, 30625 Hannover, Germany

[2] Department of Nephrology, Helios Hospital Erfurt, Erfurt, Germany

[3] Medical Clinic V, Teaching Hospital Braunschweig, Braunschweig, Germany

Published online: 12 January 2016

retention of waste products and fluid overload, treatment and outcome differ significantly depending on the cause of AKI. Kidney morphology can provide important information regarding the underlying cause.

Renal biopsy, the gold standard for evaluation of kidney morphology in renal failure, is an invasive procedure that is not feasible in all patients and has potential for complications. For this reason, alternative assessments of kidney morphology using imaging techniques are preferred methods for primary evaluation of AKI. The most accepted imaging modality for initial evaluation of renal failure is renal ultrasound, which provides valuable information with respect to kidney morphology and perfusion [2]. The major strengths of renal ultrasound are detection of obstruction and the differentiation between acute and chronic kidney diseases. Kidney size and shape, parenchymal thickness and cortical echogenicity differ significantly between these two entities [3, 4]. The utility of ultrasound in the assessment of intrinsic causes of AKI (e.g., nephrotoxic agents, infections, tubulointerstitial diseases or acute glomerulonephritis) is more variable with less sensitivity and specificity [5]; however, information on parenchymal structure and echogenicity provides some useful clues. The use of Doppler ultrasound with evaluation of the large kidney vessels and measurement of the renal resistance indices (RI) in segmental and arcuate arteries provides additional information on the cause and prognosis of AKI [6, 7]. The ultrasound characteristics of different types of AKI have recently been characterized and described in depth by Faubel et al. [8]. However, this study did not include patients with hemolytic-uremic syndrome (HUS).

During the 2011 German epidemic of HUS caused by EHEC O104:H4, we performed abdominal ultrasound examination in 41 patients with EHEC–HUS at the time of hospital admission and during follow-up. We assessed kidney morphology and perfusion and quantitated kidney parenchymal density and echogenicity by computer-based image analysis. In addition, we screened the patients for other abnormalities such as hepatosplenomegaly, pleural effusion and ascites. Findings were assessed in relationship to severity of AKI and compared to patients with other causes of AKI and healthy controls.

Methods

Patients

EHEC–HUS was diagnosed if a patient had a history of bloody diarrhea and microbiologic evidence for EHEC infection (stool cultures positive for *E. coli* producing Shiga toxin 2 (PCR and/or enzyme immunoassay) between May–July 2011 and fulfilled all of the following three criteria: (1) thrombocytopenia ($<150 \times 10^9$/L), (2) microangiopathic hemolytic anemia lactate dehydrogenase (LDH >240 U/L and hemoglobin <12.0 g/dL) and (3) acute kidney injury according to the AKIN definition. Treatment strategy was dependent on disease severity (laboratory signs of hemolysis, thrombocytopenia, peak creatinine level, need for dialysis, neurological symptoms, frequency of seizures) and included best supportive care, the use of therapeutic plasma exchange and the application of eculizumab, a humanized anti-C5 monoclonal antibody that inhibits terminal complement activation. The decision to initiate hemodialysis treatment was made on an individual basis by the physician in charge. Criteria to initiate dialysis included volume overload, symptoms of uremia, hyperkalemia and severe acidosis.

All patients who were admitted to the Department of Nephrology and Hypertension at the Hannover Medical School with suspected EHEC-associated HUS during the 2011 epidemic ($n = 54$) had a routine abdominal ultrasound examination at the time of hospital admission. This included assessment of kidney morphology and intrarenal resistance index (RI) by Doppler ultrasound as well as screening for other abnormalities (hepatomegaly, splenomegaly, ascites, pleural effusion). This ultrasound examination was performed as clinical routine assessment as standard of clinical care.

Therefore, quality of stored ultrasound images was variable (depending on the ultrasound machine that was used for examination) and not suitable for retrospective analysis in all cases; for this reason, 12 patients were excluded from our analysis. One additional patient was excluded from this analysis because EHEC infection or HUS was not confirmed. All remaining patients ($n = 41$) were included in this analysis. Twenty-one of these patients had a routine abdominal ultrasound at the follow-up visit in our outpatient clinic after recovery (6 ± 2 weeks after admission). The decision for the ultrasound examination at follow-up was at the discretion of the attending physician. A flowchart of the patients and data available for analysis is shown in Fig. 1. The study was carried out according to the Declaration of Helsinki and approved by the institutional review board at Hannover Medical School; due to the retrospective nature of the analysis that used only anonymized parameters that were obtained for routine clinical assessments, no individual written consent was required.

Patients with other causes of acute kidney injury (AKI) served as controls. We included patients who had a kidney ultrasound for evaluation of acute renal failure between August 2012 and June 2013. Patients were excluded if they had preexisting chronic renal insufficiency or known liver disease, leaving $n = 42$ patients with AKI as the control group. Reasons for AKI were: prerenal AKI (circulatory/ischemic) ($n = 13$) (31 %), non-renal transplant-associated

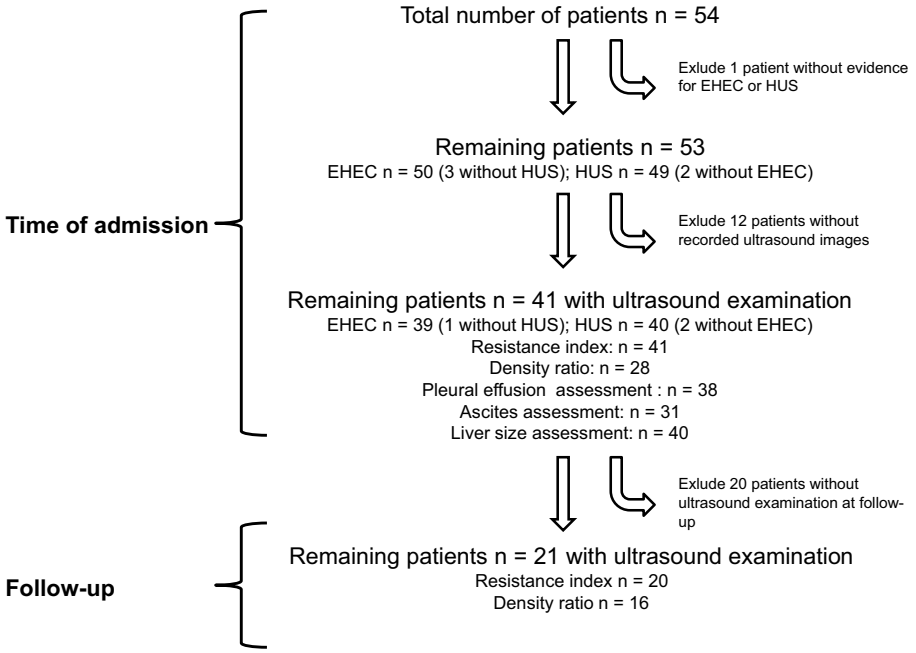

Fig. 1 Flowchart of patients included in the study for different aspects of analysis. This study was performed as a retrospective analysis of routine clinical assessments rather than being planned as a controlled prospective study. Therefore, not all assessments are available for all patients, and patient numbers vary for different assessments. This flowchart gives an overview of the data that were available and used for analysis

AKI ($n = 6$) (14 %), sepsis ($n = 3$) (7 %), intrarenal AKI ($n = 7$) (17 %), drug toxicity ($n = 6$) (14 %), postrenal AKI $n = 4$ (10 %), unclear/multifactorial ($n = 3$) (7 %). Additional control groups were recruited from patients with biopsy-proven atypical HUS (aHUS) ($n = 8$), biopsy-proven glomerulopathy ($n = 18$) and healthy controls ($n = 19$).

Diagnoses in the glomerulopathy group were antineutrophilic antibody-associated vasculitis ($n = 8$), lupus nephritis ($n = 3$), membranoproliferative glomerulonephritis ($n = 2$), focal segmental glomerulosclerosis ($n = 4$) and minimal change glomerulonephritis ($n = 1$).

Quantification of renal morphology and parenchymal density

Kidney size was assessed based on volume (calculated by the ellipsoid formula: volume = length × height × width × 0.49). Normal size is assumed when the kidney volume (in cm^3) is within the following range: patient's weight (kg) × 2 ± 20 % [9].

For assessment of the RI, we took two measurements of RI for each kidney (upper and lower pole) and used the average of these measurements in each kidney for our analysis.

For quantification of parenchymal density, we performed a computer-based image analysis of the kidney parenchyma and the liver parenchyma using gray intensity values. Due to the retrospective design of this study, we could only include a subset of EHEC–HUS patients in whom quality of recorded images was suitable for this analysis ($n = 28$). The control groups were recruited prospectively; thus, all of these control patients were included in this analysis [patients with other causes of AKI ($n = 42$), biopsy-proven aHUS ($n = 8$), biopsy-proven glomerulopathy ($n = 18$) and healthy controls ($n = 19$)]. Measurements were obtained using the software ImageJ (http://imagej.nih.gov/). For each patient, we obtained 10 kidney and liver measurements each from two separate ultrasound images. For standardization of measurements and reduction in technical variability, we calculated the ratio between average kidney and liver intensity values for each image. Image analysis was performed independently by two physicians (AR and GE) for each patient; average values of those two assessments were used for analysis.

Data analysis

Data analysis was performed using the statistical programs SPSS and GraphPad Prism. Groups were compared by independent t test or—in case of multiple groups—using ANOVA with Dunnett's post hoc analysis; Chi-square or Fisher's exact tests were used for comparisons between groups for categorical data. The significance levels were set at 0.05 unless stated otherwise.

Results

Patient population and clinical presentation

We included $n = 41$ patients with EHEC–HUS in this analysis. A flowchart of patient selection is shown in Fig. 1. Patients with other causes of AKI ($n = 42$), patients with

Table 1 Patient demographics

	EHEC–HUS ($n = 41$)	aHUS ($n = 8$)	AKI non-EHEC ($n = 42$)	Glomerulopathy ($n = 18$)
Age	44 ± 17	31 ± 10	47 ± 18	47 ± 20
Gender (female)	26 (68 %)	5 (63 %)	14 (33 %)	8 (44 %)
Creatinine (at diagnosis)	406 ± 232 µmol/l	629 ± 400 µmol/l	309 ± 227 µmol/l	333 ± 265
Dialysis necessity	25 (61 %)	5 (63 %)	19 (45 %)	5 (28 %)
Diagnosis/cause of AKI	EHEC $n = 39$ HUS $n = 40$	aHUS $n = 8$	Prerenal (circulatory/ischemic) $n = 13$ (31 %) Non-renal transplant associated $n = 6$ (14 %) Sepsis $n = 3$ (7 %) Intrarenal AKI $n = 7$ (17 %) Drug toxicity $n = 6$ (14 %) Postrenal AKI $n = 4$ (10 %) Unclear/multifactorial $n = 3$ (7 %)	ANCA-associated vasculitis $n = 8$ (44 %) SLE associated $n = 3$ (17 %) MPGN $n = 2$ (11 %) FSGS $n = 4$ (22 %) MCGN $n = 1$ (6 %)

EHEC enterohemorrhagic *Escherichia coli*, *HUS* hemolytic-uremic syndrome, *AKI* acute kidney injury, *ANCA* antineutrophil cytoplasmatic antibody, *SLE* systemic lupus erythematodes, *MPGN* membranoproliferative glomerulonephritis, *FSGS* focal segmental glomerulosclerosis, *MCGN* minimal change glomerulonephritis

aHUS ($n = 8$), glomerulopathy ($n = 18$) and healthy volunteers ($n = 19$) served as controls. Demographics of EHEC–HUS and other patients with AKI are given in Table 1. Average age was similar across the groups (44 years in EHEC–HUS vs 47 years in AKI non-EHEC and glomerulopathy) with the exception of aHUS patients who were younger (31 ± 10). The proportion of female patients was higher in the EHEC–HUS (68 %) and aHUS (63 %) cohorts vs AKI non-EHEC (33 %) and in the glomerulopathy group (50 %), ($p < 0.00001$). Temporary dialysis treatment was necessary in 61 % of EHEC–HUS (aHUS 63 %) versus 45 % of AKI and 33 % of glomerulopathy patients ($p = 0.0004$). Effects of treatment on the EHEC–HUS patient cohort have been published elsewhere as part of a larger cohort [10, 11].

Kidney morphology in EHEC–HUS

Kidney size was increased in 28/41 EHEC–HUS patients (68 %); in the remaining patients, kidneys were not formally enlarged (see formula in the methods section) but had a swollen appearance. The parenchyma was thickened (21.9 ± 2.6 mm) and showed remarkably enhanced echogenicity of the cortex. The cortex appeared almost white compared to the decreased echogenicity of the medullary pyramids (Fig. 2a, b). In many cases, we observed an extracapsular rim of perirenal lucency ("renal sweating"). At time of follow-up, kidney size was enlarged in only 6/21 patients (29 %). Cortical thickness returned to normal (18.3 ± 2.4 mm, $p < 0.001$); echogenicity of the renal cortex decreased and was comparable to the liver parenchyma (Fig. 2c).

Intrarenal resistance index (RI)

Patients with EHEC–HUS showed high intrarenal resistance index values (RI) (0.80 ± 0.08). This is a common finding in patients with AKI; however, RI values in patients with EHEC–HUS were significantly higher than in patients with aHUS (0.68 ± 0.07, $p < 0.001$), AKI due to glomerulopathy (0.68 ± 0.08, $p < 0.001$) or other causes of AKI (0.74 ± 0.10, $p < 0.01$) (Fig. 3a). After recovery of renal function, RI values decreased significantly in EHEC–HUS patients ($p < 0.001$). However, despite the statistically significant difference, there is large overlap in RI values between patients with EHEC–HUS and patients with AKI due to causes other than glomerulopathy. In the EHEC–HUS cohort, RI values were higher in patients with dialysis-dependent renal failure ($n = 25$) than in patients who did not require dialysis ($n = 16$) (0.82 ± 0.07 vs 0.76 ± 0.09; $p = 0.019$) (Fig. 3b). At time of follow-up, RI returned to normal, independent of previous dialysis dependency [dialysis ($n = 13$): RI = 0.64 ± 0.05; no dialysis ($n = 6$): RI = 0.64 ± 0.04].

Kidney/liver intensity ratio

The kidney parenchyma in EHEC–HUS patients showed a remarkably enhanced density that is not usually observed to this extent in AKI. For quantification of parenchymal density, we performed a computer-based image analysis (Fig. 2d). Kidney density measurements were normalized to liver density values in order to account for variability in ultrasound settings.

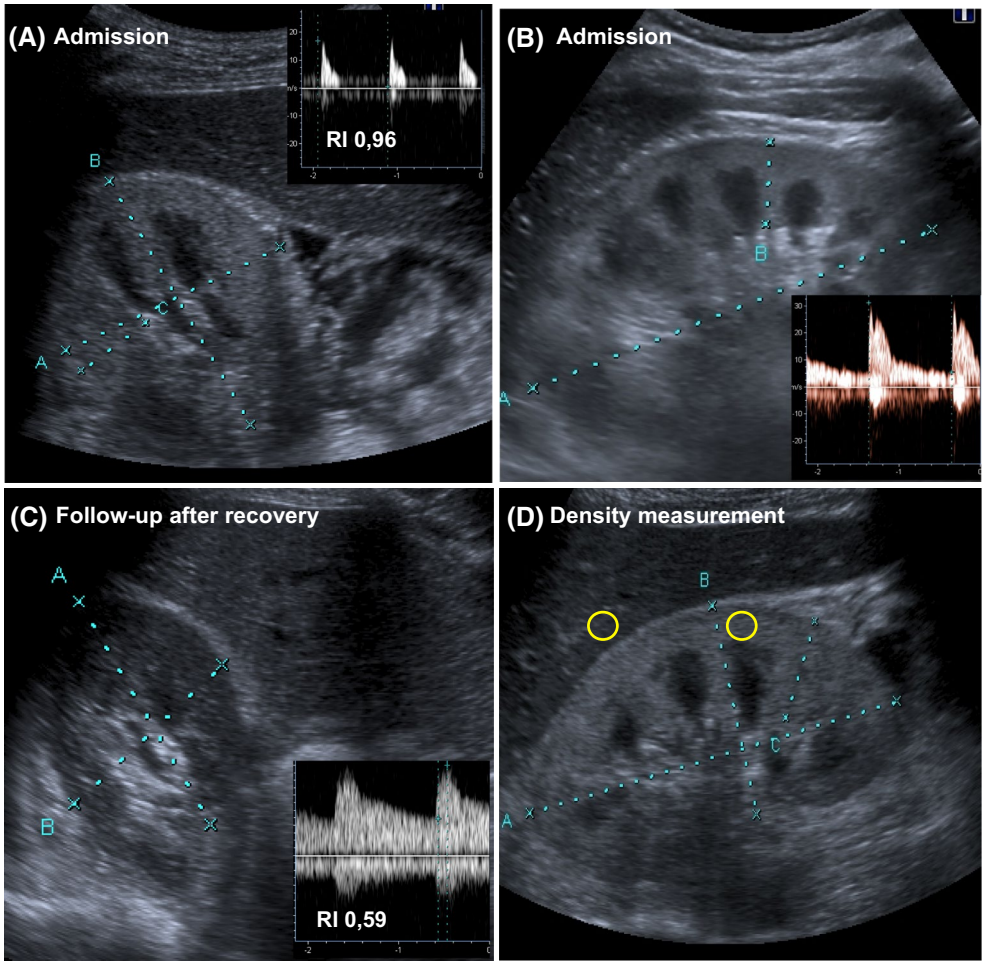

Fig. 2 Renal morphology in EHEC–HUS patients. **a**, **b** Kidneys in EHEC–HUS patients were swollen and showed remarkable echogenicity of the cortex; the cortex appeared almost white compared to the decreased echogenicity of the medullary pyramids. In many cases, we observed an extracapsular rim of perirenal lucency ("kidney sweat"). **c** After recovery, echogenicity of the renal cortex decreased and was comparable to the liver parenchyma. **d** Kidney parenchymal density was quantitated using a computer-based image analysis algorithm

Patients with AKI showed increased kidney parenchymal density (i.e., kidney/liver intensity ratios) compared to healthy controls, regardless of the cause of AKI (Fig. 3c). However, patients with EHEC–HUS or aHUS had significantly higher density ratio values (1.39 ± 0.35 or 1.43 ± 0.37) compared to patients with AKI due to glomerulopathy (1.18 ± 0.20, $p < 0.05$), patients with other causes of AKI (1.12 ± 0.21, $p < 0.001$) and healthy controls (0.86 ± 0.16, $p < 0.001$) (Fig. 3c). Only patients with cast nephropathy ($n = 4$) showed increased echogenicity (1.51 ± 0.06) similar to patients with EHEC–HUS ($p = 0.5$) (data not shown). ROC curve analysis illustrates the discrimination between patients with EHEC–HUS and patients with AKI due to glomerulopathy or other causes of AKI using parenchymal density measurement (Fig. 4). ROC curves were significant for discrimination between EHEC–HUS and all other causes of AKI (including glomerulopathy and aHUS) [AUC = 0.70 (95 % CI 0.58–0.83); $p = 0.002$] (Fig. 4a), EHEC–HUS and patients with AKI due to causes other than glomerulopathy or aHUS [AUC = 0.75 (95 % CI 0.62–0.88), $p < 0.001$] (Fig. 4b), EHEC–HUS and patients with glomerulopathy [AUC = 0.69 (95 % CI 0.54–0.85); $p = 0.028$] (Fig. 4c). There was no discrimination between patients with EHEC–HUS and those with aHUS [AUC = 0.49 (95 % CI 0.26–0.73); $p = 0.954$] (Fig. 4d). In contrast to EHEC–HUS, there was no difference in parenchymal density in kidneys with AKI due to glomerulopathy compared to those with other non-HUS causes of AKI. Interestingly, the patient with the highest density value in the non-HUS AKI patient group was diagnosed with thrombotic microangiopathy of unknown cause, supporting the hypothesis that the striking increase in parenchymal echogenicity in EHEC–HUS and aHUS

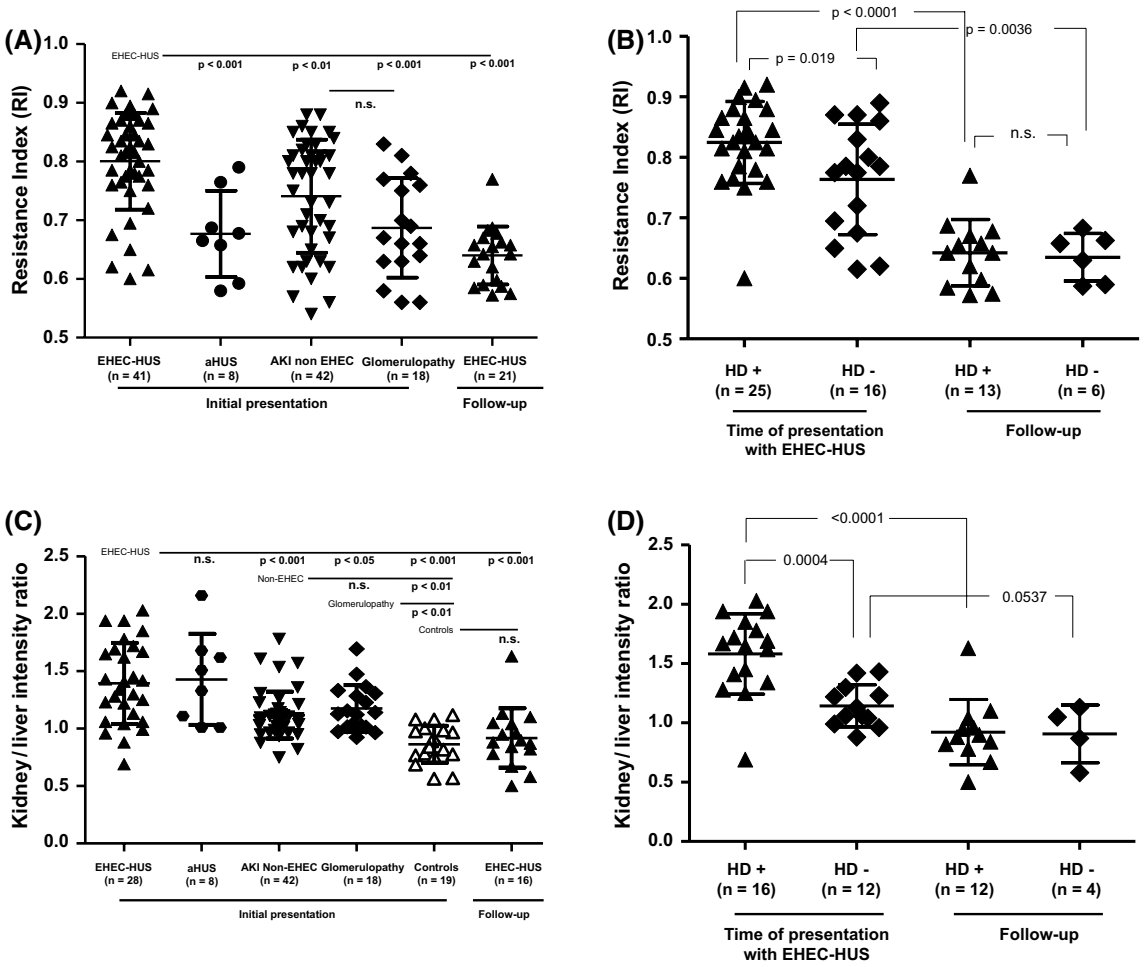

Fig. 3 Renal resistance index (RI) and density measurements in patients with EHEC–HUS and other causes of acute kidney injury (AKI). **a** We compared the renal resistance index in patients with EHEC–HUS to patients with other causes of AKI. **b** We assessed the relationship between the renal resistance index and the necessity for hemodialysis at the time of hospital admission and during follow-up in patients with EHEC–HUS. **c** We analyzed the kidney/liver density ratio in patients with HUS compared to other causes of AKI at the time of hospital admission. **d** We assessed the relationship between the kidney/liver ratio and severity of renal functional impairment (represented by the necessity for hemodialysis). *Error bars* represent standard deviation

is related to the microangiopathic pathophysiology of AKI.

The extent of parenchymal echogenicity in the EHEC–HUS patients correlated with severity of renal dysfunction: the kidney/liver density ratio was higher in EHEC–HUS patients who required dialysis treatment ($n = 16$) (1.58 ± 0.34) compared to those without dialysis ($n = 12$) (1.14 ± 0.18, $p = 0.0004$) (Fig. 3d). ROC curve analysis suggests that the density assessment supports the distinction between patients with EHEC–HUS that will require dialysis from those who will not [AUC = 0.885 (95 % CI 0.693–1.00), $p = 0.001$].

After recovery, kidney parenchymal density in EHEC–HUS patients ($n = 16$) (0.92 ± 0.27) returned to levels of healthy controls ($n = 19$) (0.86 ± 0.16), regardless of the prior need for dialysis.

Density measurements showed high reproducibility with high correlation between assessments of two independent observers ($r^2 = 0.701$, $p < 0.001$) (Fig. 5).

Extrarenal ultrasound findings

A significant proportion of EHEC–HUS patients showed pathological findings beyond signs of acute kidney injury, including hepatomegaly (45 %), splenomegaly (39 %), ascites (84 %) and pleural effusions (61 %) (Fig. 6a). Ascites and pleural effusion were significantly more common in patients with EHEC–HUS compared to patients with glomerulopathy [ascites 14 % ($p < 0.001$), pleural effusions 17 % ($p < 0.001$)] and patients with other causes of AKI [ascites 38 % ($p = 0.002$), pleural effusion 45 % ($p = 0.002$)] (Fig. 6a).

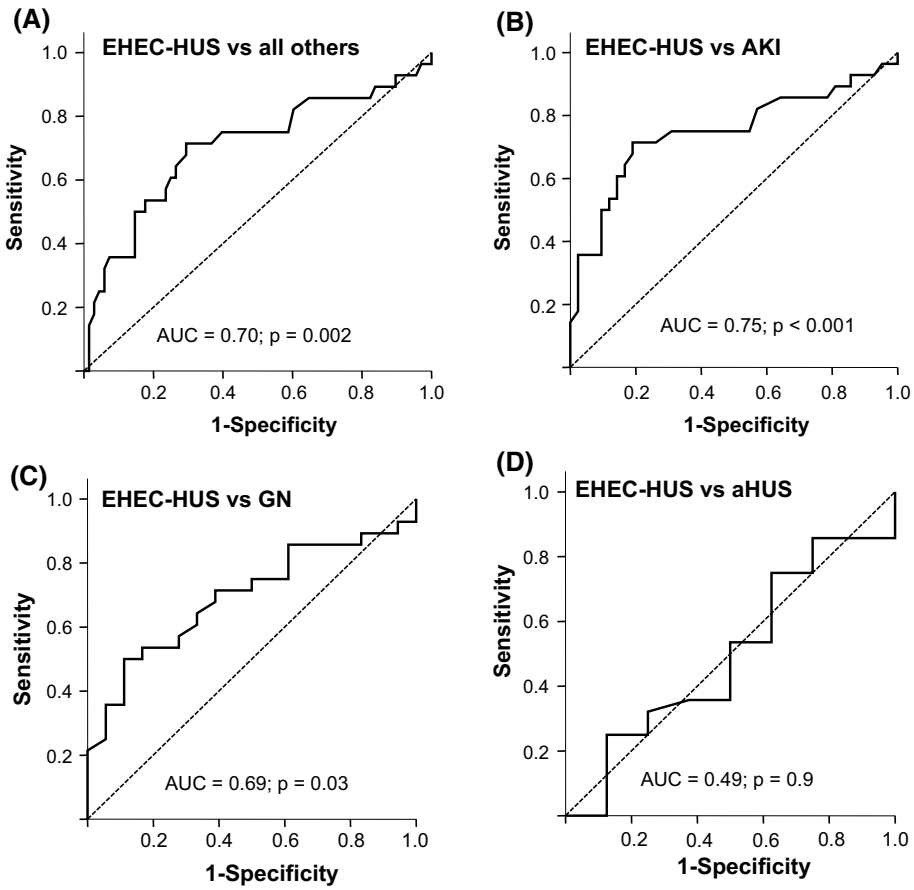

Fig. 4 Sensitivity and specificity of kidney density measurement. We performed ROC curve analysis to assess the ability to discriminate between patients with EHEC–HUS and **a** patients with other causes of acute renal failure (aHUS, glomerulopathy or other causes of AKI), **b** patients with AKI due to causes other than glomerulopathy or aHUS, **c** patients with glomerulopathy (GN) and **d** patients with aHUS

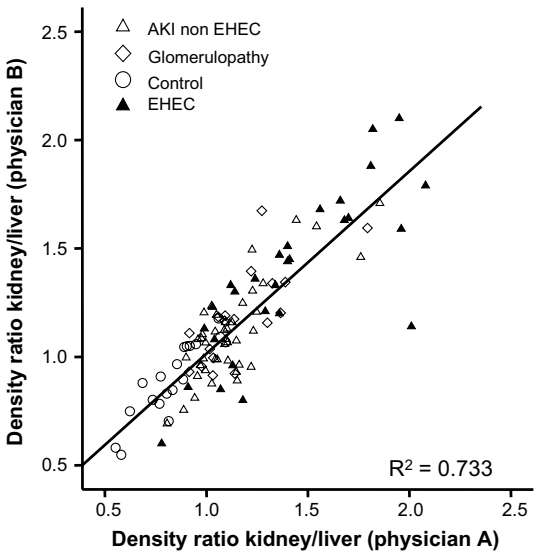

Fig. 5 Reliability of the kidney/liver density ratio for assessment of kidney injury. To ensure robustness of the measurements, assessment of the density ratio was performed independently by two physicians on two images each. The average score for each physician is plotted for each patient

Due to the significant proportion of patients with hepatomegaly in EHEC–HUS, we considered whether changes in the liver parenchymal density might be responsible for the changes in the liver/kidney density ratios in the EHEC–HUS patients. However, there was no relationship between the kidney/liver intensity ratios and liver function tests (Fig. 6b) or the presence or absence of hepatomegaly (Fig. 6c). Thus, changes in the intensity ratios are not related to alterations in the liver parenchyma, but have to be attributed to kidney injury and associated changes in kidney morphology.

There was no significant relationship between the presence of pleural effusion and the necessity for dialysis (Fig. 6d), indicating that these findings are not simply an indication of volume overload but represent independent extrarenal manifestations of EHEC/HUS.

Discussion

Patients with EHEC–HUS had a characteristic constellation of morphologic abnormalities on ultrasound examination

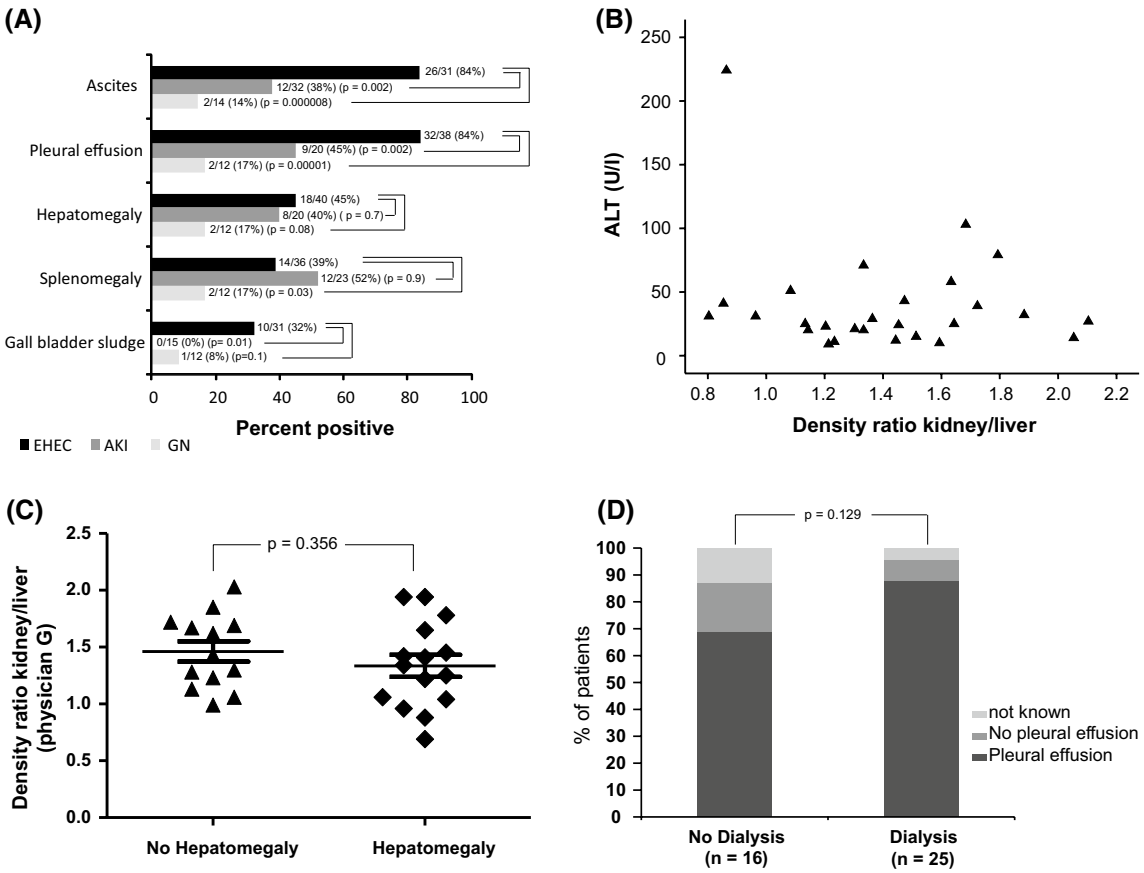

Fig. 6 Extrarenal ultrasound findings in patients with EHEC–HUS. The morphologic abnormalities in EHEC–HUS patients were not only limited to the kidney but also included ascites, pleural effusion, hepatomegaly, splenomegaly and significant gall bladder sludge. **a** This panel shows the prevalence of these extrarenal abnormalities. **b**, **c** Due to our normalization of the density assessment using liver parenchymal density for standardization and reduction in technical variability, it is possible that variability in liver density could have a significant effect on the liver/kidney density ratio in this patient cohort. We therefore assessed the relationship between liver density measurements and liver function tests (**b**) or hepatomegaly (**c**). **d** To assess whether the pleural effusion was an effect of volume overload or an independent pathological finding, we assessed the relationship between the presence of pleural effusion and the necessity for hemodialysis

with striking changes in kidney morphology including high parenchymal echogenicity and severely impaired kidney perfusion. The extent of changes in kidney morphology was related to the clinical severity of AKI (assessed by the need for temporary dialysis). After clinical recovery, kidney morphology returned to values of healthy controls. In addition to renal changes, the majority of patients also showed extrarenal abnormalities such as hepato-splenomegaly, pleural effusion and ascites.

We standardized the quantification of parenchymal echogenicity by using the kidney/liver density ratio to minimize the influence of technical variability. The use of liver parenchyma for standardization is not unproblematic and limited by concomitant disease such as steatosis hepatis [8], since changes in liver parenchymal density would influence the density ratio. However, the patients in our EHEC–HUS cohort were otherwise healthy and had no significant disease; in the control group, we excluded patients with morphologic signs of steatosis hepatis. Furthermore, the ratios were calculated within each image for each patient. Within the follow-up period of 6 weeks for individual patients (with no known liver disease), it is unlikely that there would be significant changes to the liver parenchyma; thus, we are confident that the observed changes in ratios in the follow-up measurements of EHEC–HUS patients can be attributed to changes in kidney parenchymal density rather than being influenced by alterations in the liver parenchyma.

Due to the acute onset of the EHEC epidemic, this study was not performed as a systematic prospective evaluation but rather as a retrospective analysis of diagnostic procedures obtained during a medical crisis. Ultrasound examinations were performed in an emergency setting; therefore, we could not always achieve optimal image quality

and included only patients for whom images of adequate quality were available. Due to the nature of EHEC–HUS disease, which manifested almost exclusively in otherwise healthy younger adults, we could not match our control group of non-HUS AKI for concomitant disease. As is common in clinical practice, most patients with AKI (including patients with EHEC–HUS) were not biopsied if the cause of deterioration in kidney function could be determined with sufficient certainty based on clinical features. Especially patients with HUS have a high risk of complications after the biopsy (e.g., due to thrombocytopenia). However, the clinical picture of EHEC–HUS is very typical (diarrhea, hemolysis, low platelet count, acute renal failure). In addition, we had microbiologic evidence for EHEC infection in 39/41 patients (95 %). Therefore, even without a biopsy, we are certain about the diagnosis of EHEC–HUS in these patients. However, to our knowledge, our report describes by far the largest adult patient cohort with EHEC-associated HUS and is the only analysis in these patients that uses an objective, quantitative and highly reproducible assessment of parenchymal echogenicity to assess renal morphology in relationship to severity and cause of AKI.

The observed increase in echogenicity with swelling of the renal parenchyma in patients with EHEC–HUS was striking. Our results confirm previous reports that showed markedly increased echogenicity in EHEC-associated HUS by B-mode ultrasound examination [12–14] and significantly reduced diastolic blood flow, implicating a high RI, by color Doppler in children with HUS [15, 16]. The most common clinical use of assessment of kidney morphology is in the assessment of chronicity of kidney disease, where high echogenicity and high RI values in combination with reduced parenchymal thickness provide useful clues for differentiating chronic from acute renal failure [4]. In contrast, morphology in the setting of AKI has limited value in the diagnosis of the underlying disease, since increased echogenicity of the renal cortex is a feature of many causes of AKI (HIV-associated renal failure, Lupus nephritis, hemolytic-uremic syndrome and nephrotoxic AKI) [14, 17–19]. Studies comparing kidney biopsy findings with renal morphology on ultrasound examination could not find disease-specific changes [20]. Thus, there is no specificity of increased echogenicity for certain causes of AKI [3, 5, 8]. In our study, patients with EHEC–HUS-associated AKI had higher parenchymal echogenicity than patients with other causes of AKI. These striking morphologic changes are probably related to the underlying pathophysiological mechanisms. High parenchymal echogenicity is associated with histologic findings of glomerular casts, interstitial inflammation and interstitial edema [21–23]. HUS is associated with endothelial swelling, subendothelial aggregation of material and hyaline microthrombi of arterioles and capillaries [24–26]. It is conceivable that the increased RI and the remarkably increased echogenicity in EHEC–HUS are caused by these disease-specific detrimental renal alterations. This assumption is supported by the fact that the highest echogenicity in the non-EHEC patients with AKI was seen in a patient with biopsy-proven thrombotic microangiopathy. Ultrasound examination and assessment of parenchymal echogenicity thus can be used as one additional marker in the clinical routine to support a diagnosis of HUS in patients with otherwise suspicious clinical symptoms. Similarly, low parenchymal echogenicity should prompt a physician to consider alternative diagnoses if HUS is suspected based on clinical symptoms (e.g., thrombocytopenia in septic shock). However, it should be kept in mind that increased echogenicity is a quantitative marker and has no absolute specificity for HUS; therefore, results of the ultrasound examination should always be interpreted in the context of other clinical findings.

In addition to the diagnostic information, the alterations in kidney morphology and perfusion also had prognostic value. We found that the severity of parenchymal morphologic changes and perfusion in the kidney at the time of hospital admission correlated with the necessity for dialysis during the further course of disease and thus has prognostic value. Results in previous reports of B-mode ultrasound assessment in children with EHEC–HUS provided evidence for a relationship between increase in kidney echogenicity and the clinical course of disease [12, 13]. However, the analysis by Choyke et al. [12] was performed in a different clinical setting (small cohort of very young children under the age of 5 years). The analysis of Glatstein et al. [13] did not quantitate the severity of morphologic changes and therefore does not provide quantitative measurements for prognostic evaluation in this disease. The quantitative and objective assessment of echogenicity using image analysis in our study was highly reproducible and confirmed a relationship between intensity of morphologic changes and severity of AKI with necessity for dialysis and thus adds not only diagnostic but also prognostic value to the assessment by B-mode ultrasound.

The presence of extrarenal abnormalities (hepatosplenomegaly, pleural effusion, ascites) was common in EHEC–HUS patients, but was not related to the necessity for dialysis treatment, indicating that these findings are an independent manifestation of disease and not simply an indication of volume overload due to severely impaired kidney function. Our observations confirm findings of other authors that have described an increased incidence of pleural effusion in children with HUS-associated AKI compared to other etiologies of AKI [27]. Possible mechanisms include Shiga toxin-associated cardiac dysfunction [28] including pericardial effusion [29] and systemic endothelial injury caused by Shiga toxin [30], resulting in systemic capillary leak. We assume that this capillary leak is also the

cause of the hepato-splenomegaly observed in a significant proportion of EHEC–HUS patients.

We conclude that B-mode and Doppler sonography might be a helpful tool to verify the diagnosis in clinically suspected HUS and thrombotic microangiopathies. Due to the highly echogenic kidney in combination with increased RI and signs of capillary leak, the sonographic presentation of this disease differs from other forms of AKI. This could be favorable in situations where thrombocytopenia, which is not only seen in HUS but also in hematological disorders, septic shock and DIC, prevents performance of a diagnostic renal biopsy. In these patients, ultrasound morphology can be used as an additional clinical parameter in the context of other clinical features to support the diagnostic process. Additionally, the relationship of the measurements with severity and clinical course of clinical renal disease implicates a prognostic value in future patient evaluation.

Acknowledgments The authors thank Katharina Wenzig for assistance in patient recruitment and ultrasound examinations.

Compliance with ethical standards

Conflict of interest The authors have no conflict of interest relevant to this study.

References

1. Waikar SS, Liu KD, Chertow GM (2008) Diagnosis, epidemiology and outcomes of acute kidney injury. Clin J Am Soc Nephrol 3(3):844–861
2. Bush WH Jr, Amis ES Jr, Bigongiari LR et al (2000) Radiologic investigation of causes of renal failure. American College of Radiology. ACR Appropriateness Criteria. Radiology 215(Suppl):713–720
3. O'Neill WC (2000) Sonographic evaluation of renal failure. Am J Kidney Dis 35(6):1021–1038
4. Ozmen CA, Akin D, Bilek SU, Bayrak AH, Senturk S, Nazaroglu H (2010) Ultrasound as a diagnostic tool to differentiate acute from chronic renal failure. Clin Nephrol 74(1):46–52
5. O'Neill WC (2006) B-mode sonography in acute renal failure. Nephron Clin Pract 103(2):c19–c23
6. Izumi M, Sugiura T, Nakamura H, Nagatoya K, Imai E, Hori M (2000) Differential diagnosis of prerenal azotemia from acute tubular necrosis and prediction of recovery by Doppler ultrasound. Am J Kidney Dis 35(4):713–719
7. Schnell D, Darmon M (2012) Renal Doppler to assess renal perfusion in the critically ill: a reappraisal. Intensive Care Med 38(11):1751–1760
8. Faubel S, Patel NU, Lockhart ME, Cadnapaphornchai MA (2014) Renal relevant radiology: use of ultrasonography in patients with AKI. Clin J Am Soc Nephrol 9(2):382–394
9. Radermacher J (2005) Ultrasonography of the kidney and the renal vessels. I. Normal findings, inherited and parenchymal diseases. Urologe A 44(11):1351–1363
10. Menne J, Nitschke M, Stingele R et al (2012) Validation of treatment strategies for enterohaemorrhagic *Escherichia coli* O104:H4 induced haemolytic uraemic syndrome: case–control study. BMJ 345:e4565
11. Kielstein JT, Beutel G, Fleig S et al (2012) Collaborators of the DGfN STEC-HUS registry. Best supportive care and therapeutic plasma exchange with or without eculizumab in Shiga-toxin-producing *E. coli* O104:H4 induced haemolytic-uraemic syndrome: an analysis of the German STEC-HUS registry. Nephrol Dial Transplant 27(10):3807–3815
12. Choyke PL, Grant EG, Hoffer FA, Tina L, Korec S (1988) Cortical echogenicity in the hemolytic uremic syndrome: clinical correlation. J Ultrasound Med 7(8):439–442
13. Glatstein M, Miller E, Garcia-Bournissen F, Scolnik D (2010) Timing and utility of ultrasound in diarrhea-associated hemolytic uremic syndrome: 7-year experience of a large tertiary care hospital. Clin Pediatr (Phila) 49(5):418–421
14. Kenney PJ, Brinsko RE, Patel DV, Spitzer RE, Farrar FM (1986) Sonography of the kidneys in hemolytic uremic syndrome. Invest Radiol 21(7):547–550
15. Patriquin HB, O'Regan S, Robitaille P, Paltiel H (1989) Hemolytic-uremic syndrome: intrarenal arterial Doppler patterns as a useful guide to therapy. Radiology 172(3):625–628
16. Scholbach TM (2001) Changes of renal flow volume in the hemolytic-uremic syndrome–color Doppler sonographic investigations. Pediatr Nephrol 16(8):644–647
17. Di Fiori JL, Rodrigue D, Kaptein EM, Ralls PW (1998) Diagnostic sonography of HIV-associated nephropathy: new observations and clinical correlation. AJR Am J Roentgenol 171(3):713–716
18. Rosenfield AT, Zeman RK, Cicchetti DV, Siegel NJ (1985) Experimental acute tubular necrosis: US appearance. Radiology 157(3):771–774
19. Stanley JH, Cornella R, Loevinger E, Schabel SI, Curry NS (1984) Sonography of systemic lupus nephritis. AJR Am J Roentgenol 142(6):1165–1168
20. Paivansalo M, Huttunen K, Suramo I (1985) Ultrasonographic findings in renal parenchymal diseases. Scand J Urol Nephrol 19(2):119–123
21. Hricak H, Cruz C, Romanski R et al (1982) Renal parenchymal disease: sonographic-histologic correlation. Radiology 144(1):141–147
22. Moghazi S, Jones E, Schroepple J et al (2005) Correlation of renal histopathology with sonographic findings. Kidney Int 67(4):1515–1520
23. Rosenfield AT, Siegel NJ (1981) Renal parenchymal disease: histopathologic-sonographic correlation. AJR Am J Roentgenol 137(4):793–798
24. Benz K, Amann K (2009) Pathological aspects of membranoproliferative glomerulonephritis (MPGN) and haemolytic uraemic syndrome (HUS)/thrombocytic thrombopenic purpura (TTP). Thromb Haemost 101(2):265–270
25. Inward CD, Howie AJ, Fitzpatrick MM, Rafaat F, Milford DV, Taylor CM (1997) Renal histopathology in fatal cases of diarrhoea-associated haemolytic uraemic syndrome. British Association for Paediatric Nephrology. Pediatr Nephrol 11(5):556–559
26. Noris M, Remuzzi G (2009) Atypical hemolytic-uremic syndrome. N Engl J Med 361(17):1676–1687
27. Butani L, Polinsky MS, Kaiser BA, Baluarte HJ (1998) Pleural effusion complicating acute peritoneal dialysis in hemolytic uremic syndrome. Pediatr Nephrol 12(9):772–774
28. Tarr PI, Gordon CA, Chandler WL (2005) Shiga-toxin-producing *Escherichia coli* and haemolytic uraemic syndrome. Lancet 365(9464):1073–1086
29. Mohammed J, Filler G, Price A, Sharma AP (2009) Cardiac tamponade in diarrhoea-positive haemolytic uraemic syndrome. Nephrol Dial Transplant 24(2):679–681
30. Petruzziello-Pellegrini TN, Marsden PA (2012) Shiga toxin-associated hemolytic uremic syndrome: advances in pathogenesis and therapeutics. Curr Opin Nephrol Hypertens 21(4):433–440